Modeling Hazardous Gas Dispersion in Neutrally and Stably Stratified Atmospheric Boundary Layer Flows

Ramechecandane, S and Eswari, N
[1]System Engineer, [2]Cost Engineer
FMC Technologies, NO-3601, Kongsberg, Norway
E-mail: remechecandan.somassoundirame@fmcti.com

ABSTRACT

The objective of the present work is to propose a methodology to simulate hazardous gas dispersion in neutrally and stably stratified atmospheric boundary layer (ABL) flows. The profiles of velocity, temperature and turbulence quantities are set based on the stratification effect. Special emphasis is placed on the generation of a horizontally homogeneous turbulent boundary layer (HHTBL). FLUENT software is validated for simulating ABL flows by comparing the results obtained with available numerical data from the literature. The fully developed profiles of velocity, turbulent kinetic energy, turbulent dissipation rate and temperature are implemented as user defined functions in the commercial code FLUENT. The hazardous gas release is modeled using the convection diffusion equation. Four test cases from the classical Prairie Grass experiment are considered for validating the present approach. The predicted concentration of the SO_2 gas at various locations of the test field (50, 100, 200, 400 and 800 m) are in close agreement with the experimental data. The cases of neutral stratification compare quite well with the experimental data and there exist a slight discrepancy in the stably stratified cases. This mismatch can be attributed to measurement errors and the anisotropic nature of the ABL flows.

1. INTRODUCTION

Modeling the dispersion of hazardous pollutants and gases in an urban atmosphere has remained as a challenging area of research for the past few decades. With the advent of modern computers and the consistent increase of computational power, the task of computationally modeling the atmospheric boundary layers (ABL)/Planetary boundary layers (PBL) and the dispersion of hazardous gases have become totally viable. Modeling the earth's atmosphere is among the most difficult tasks that a computational fluid dynamics code has to handle. The velocity components, turbulent quantities and the temperature keeps changing rapidly and thereby makes the computational work a lot more horrendous. The simplest assumption that one would make while tackling such a problem is to consider the flow to be steady or quasi-steady in nature.

Modeling the transient behavior of the atmosphere is not far from imagination and is considered to be normal to perform studies for shorter durations to capture intricate flow features. The CFD analysis of ABL flows are performed by solving the Reynolds Averaged Navier-Stokes equations (RANS) or Large Eddy Simulations (LES). From a computational stand point, the RANS approach is more desirable owing to its robustness, simplicity and lower computational cost. With Reynolds averaging the number of unknowns increase in the form of Reynolds stresses and the closure of these set of equations turns out to be difficult. There exist a number of turbulence models to achieve closure of the RANS set of equations and the choice of the turbulence models for a particular application depends truly on past experience. The two equation turbulence models [1–4] are among the most widely used for predicting ABL flows. The k-ε model has been applied for modeling ABL flows and to simulate hazardous gas dispersion successfully in the past [5, 6]. The inherent disadvantage in a two equation model is that the anisotropicity of turbulence cannot be captured using these models. The Reynolds Stress Model (RSM) or the Large Eddy Simulation (LES) can resolve the anisotropic effects but comes with a penalty of increased computation time.

Structure of ABL varies over a diurnal cycle. On a sunny day, the earth surface gets heated and the boundary layer becomes unstable, promoting convective plumes and turbulent mixing. On a clear night, the surface is cooled and the boundary layer becomes stable, suppressing vertical movement of air parcels. Though the availability of literature on modeling neutral atmospheric boundary layers is quite vast, the literature on stably and unstably stratified ABL flows is quite limited [7]. The atmospheric stability plays a pivotal role on the dispersion of pollutants, spread of wildfires, urban heat island formation and so on. The atmospheric stability may either encourage or suppress vertical air motion. The atmospheric stability greatly influences the dispersion of pollutants. For example, winds tend to be turbulent and gusty when the atmosphere is unstable and thereby enhances the dispersion of pollutants considerably. The concentration of pollutants at various locations in the downstream direction depends totally on the stratification of the atmospheric boundary layer. The neutral and stable stratifications are the most used when assessing the consequences of industrial accidents. The profiles of temperature, velocity and turbulent quantities must be representative of the atmospheric physics, in order to describe carefully the gas dispersion.

The objective of the present study is to implement the profiles of temperature, velocity and turbulent quantities in FLUENT through user defined function and compare the CFD results obtained from FLUENT with available experimental and numerical data. The classical Prairie Grass experimental data are used for validating the present methodology. The concentration of SO_2 at various locations for four test cases, are compared with CFD results.

2. MATHEMATICAL MODELING

The commercial CFD software ANSYS FLUENT is used for performing the present study. FLUENT uses finite volume method for transforming the partial differential equations to a set of algebraic equations. The equations solved are the continuity, momentum and species transport to model the pollutant dispersion.

Using Reynolds averaging, the continuity and momentum equations turn out to be

$$\frac{\partial \rho}{\partial t} + \frac{\partial}{\partial x_i}\left(\rho u_i\right) = 0 \tag{1}$$

$$\frac{\partial}{\partial t}\left(\rho u_i\right) + \frac{\partial}{\partial x_j}\left(\rho u_i u_j\right) = -\frac{\partial p}{\partial x_i} + \frac{\partial}{\partial x_j}\left[\mu\left(\frac{\partial u_i}{\partial x_j} + \frac{\partial u_j}{\partial x_i} - \frac{2}{3}\delta_{ij}\frac{\partial u_i}{\partial x_j}\right)\right] + \frac{\partial}{\partial x_j}\left(-\rho u_i' u_j'\right) \tag{2}$$

The Reynolds stresses $\rho u_i' u_j'$ in the eqn. must be modeled in order to close the equation. A common method employs the Boussinesq hypothesis to relate the Reynolds stresses to the mean velocity gradients

$$-\rho u_i' u_j' = \mu_t\left(\frac{\partial u_i}{\partial x_j} + \frac{\partial u_j}{\partial x_i}\right) - \frac{2}{3}\delta_{ij}\left(\mu_t\frac{\partial u_i}{\partial x_i} + \rho k\right) \tag{3}$$

The advantage of this approach is the relatively low computational cost associated with the computation of the turbulent viscosity (μ_t). In the case of the standard k–ε model, two additional transport equations (for the turbulent kinetic energy k, and the turbulent dissipation rate ε) are solved, and μ_t is computed as a function of k and ε.

$$\frac{\partial}{\partial t}\left(\rho k\right) + \frac{\partial}{\partial x_j}\left(\rho k u_i\right) = \frac{\partial}{\partial x_j}\left[\alpha_k\left(\mu_{eff}\frac{\partial k}{\partial x_j}\right)\right] + G_k - \rho\varepsilon \tag{4}$$

$$\frac{\partial}{\partial t}\left(\rho \varepsilon\right) + \frac{\partial}{\partial x_j}\left(\rho \varepsilon u_i\right) = \frac{\partial}{\partial x_j}\left[\alpha_\varepsilon\left(\mu_{eff}\frac{\partial \varepsilon}{\partial x_j}\right)\right] + C_{1\varepsilon}G_k\frac{\varepsilon}{k} - C_{2\varepsilon}\rho\frac{\varepsilon^2}{k} - R_\varepsilon \tag{5}$$

Table 1. Constants involved in the Standard $k - \varepsilon$ model applied to model atmospheric boundary layer flows.

C_μ	$C_{1\varepsilon}$	$C_{2\varepsilon}$	α_k	α_ε	η_0	β
0.033	1.46	1.83	1.0	2.38	4.38	0.012

In order to simulate realistic atmospheric values of the turbulent kinetic energy in the surface layer, it is necessary to use the modified constant set proposed by Duynkerke P.G [8]. The constants involved in the eqns. (4) and (5) are given in table 1.

$$\mu_t = \rho C_\mu \frac{k^2}{\varepsilon} \tag{6}$$

The disadvantage of the Boussinesq hypothesis as presented is that it assumes μ_t is an isotropic scalar quantity, which is not strictly true.

$$R_\varepsilon = \frac{C_\mu \rho \eta^3 \left(1 - \frac{\eta}{\eta_0}\right)}{1 + \beta \eta^3} \frac{\varepsilon^2}{k} \tag{7}$$

Where $\eta = \frac{Sk}{\varepsilon}$; $\eta_0 = 4.38$; $\beta = 0.012$

The term G_K representing the production of turbulent kinetic energy is modeled as

$$G_k = -\rho \grave{u_i} \grave{u_j} \tag{8}$$

In FLUENT the hazardous gas release is modeled using the Advection Diffusion module (AD). In turbulent flows, the mass diffusion is computed as

$$J_{SO_2} = -\left(\rho D_{SO_2} + \frac{\mu_t}{Sc_t}\right) \nabla Y_{SO_2} \tag{9}$$

Where D_{SO_2} is the diffusion coefficient for SO_2 in the mixture, $\mu_t = \rho C_\mu \frac{k^2}{\varepsilon}$ is the turbulent viscosity, Y_{SO_2} is the mass fraction of SO_2 in the mixture, ρ is the mixture density. $Sc_t = \frac{\mu_t}{(\rho D_t)}$ is the turbulent Schmidt number, where D_t is the turbulent diffusivity. Sc_t is set to a standard value of 0.7.

2.1. Velocity profiles:

The logarithmic velocity profiles are given by

$$\bar{u}(z) = \frac{u_*}{k}\left[\mathrm{In}\left(\frac{z + z_0}{z_0}\right) - \psi_m(\zeta) + \psi_m(\zeta_0)\right] \tag{10}$$

Where, $\psi_h(\zeta) = -\frac{5z}{L}$ and $\psi_m(\zeta_0) = -\frac{5z_0}{L}$ for stable stratification

$\psi_m(\zeta)$ and $\psi_m(\zeta_0)$ tend to zero in neutral stratification as the Monin Obukhov length tends to very high values in neutral stratification $L \to \infty$

The Monin Obukhov length is an estimate of the height where the turbulent dissipation due to the buoyancy is comparable with the shear stress production of turbulence, and is given by

$$L = -\frac{\rho C_p \theta_0 u_*^3}{kgH_0} \tag{11}$$

Where H_0 is the ground sensible heat flux; u_* is the frictional velocity; θ_0 is the ground temperature and C_p is the specific heat at constant pressure.

Hence, in the case of neutral stratification

$$\bar{u}(z) = \frac{u_*}{k}\left[\text{In}\left(\frac{z+z_0}{z_0}\right)\right] \tag{12}$$

Where k is the Von-Karman's constant and it assumes a value of 0.40. The Von-Karman value may vary from 0.40 – 0.42 in literature. z is the vertical height and z_0 is the aerodynamic roughness height. The aerodynamic roughness height can be uniform or highly non-uniform based on the topography under consideration.

2.2. Temperature profiles:

$$\bar{\theta}(z) = \theta_0 + \frac{\theta_*}{k}\left[\text{In}\left(\frac{z+z_T}{z_T}\right) - \psi_h(\zeta) + \psi_h(\zeta_0)\right] \tag{13}$$

Where, $\psi_h(\zeta) = -\frac{5z}{L}$ and $\psi_h(\zeta_0) = -\frac{5z_T}{L}$ for stable stratification

The temperature θ_* is given by

$$\theta_* = -\frac{q_w^*}{\rho C_p u_*} \tag{14}$$

Where, q_w^* is the wall heat flux in W/m^2.

$\psi_h(\zeta)$ and $\psi_h(\zeta_0)$ tend to zero in neutral stratification as the Monin Obukhov length tends to very high values in neutral stratification $L \to \infty$

Hence, in the case of neutral stratification

$$\bar{\theta}(z) = \theta_0 + \frac{\theta_*}{k}\left[\text{In}\left(\frac{z+z_T}{z_T}\right)\right] \tag{15}$$

z_T is the roughness length for temperature and is usually less than the aerodynamic roughness length z_0.

2.3. Turbulent kinetic energy profiles:

$$k(z) = \frac{u_*^2}{\sqrt{C_\mu}}\sqrt{1 - \frac{\zeta}{\phi_m(\zeta)}} \quad \text{for stable stratification} \tag{16}$$

Where $\zeta = \frac{z}{L}$ and $\phi_m(\zeta) = 1 + \frac{5z}{L}$

$k(z) = \frac{u_*^2}{\sqrt{C_\mu}}$ for neutral stratification.

2.4. Turbulent dissipation rate profiles:

$$\varepsilon(z) = \frac{u_*^3}{k(z+z_0)}\phi_m(\zeta)\left[1-\frac{\zeta}{\phi_m(\zeta)}\right] \quad \text{for stable stratification} \tag{17}$$

$$\text{Where } \zeta = \frac{z}{L} \text{ and } \phi_m(\zeta) = 1+\frac{5z}{L} \tag{18}$$

$$\varepsilon(z) = \frac{u_*^3}{k(z+z_0)} \quad \text{for neutral stratification} \tag{19}$$

The momentum turbulent diffusivity is given by

$$\mu_T(z) = \frac{\rho k u_* z}{\phi_m(\zeta)} \tag{20}$$

2.5. Boundary conditions:

In the present investigations, the velocity inlet is specified as the inlet boundary condition and the profiles of velocity, temperature, turbulence kinetic energy and turbulent dissipation rate are supplied as inputs. The equations (10)–(20) have been implemented in the commercial CFD software FLUENT. Outflow condition is specified at the outlet. The velocity and the turbulent quantities are set at the top boundary and the side boundaries are specified as symmetry. The ground is set as no slip wall with a standard wall function. The sand grain roughness height is calculated from the aerodynamic roughness height using the formula

$$k_s = \frac{9.793 z_0}{C_S} \tag{21}$$

C_S can take a value of 0.5 for uniform roughness height and for non-uniform roughness heights the value approaches 1. For the present study the value of C_S is set as 9.793 based on previous studies.

3. RESULTS & DISCUSSION

3.1. Horizontally homogeneous turbulent boundary layer

The major difficulty in modeling an ABL flow is to create a developed boundary layer profile and to ensure horizontal homogeneity of the applied profile in the computational domain. The problem of horizontal homogeneity has been so widely discussed in the recent past [5–7]. In the present study due attention has been paid to the choice of boundary conditions specified and the profiles of the primitive variables applied. From the literature, it is seen that there exist a bit of discrepancy in the profiles of turbulent kinetic energy applied. In the case of neutral stratification the turbulent kinetic energy may be represented by

$$k(z) = \frac{u_*^2}{\sqrt{C_\mu}} \tag{22}$$

Or

$$k(z) = \frac{u_*^2}{\sqrt{C_\mu}}\left(1-\frac{z}{\delta}\right)^2 \tag{23}$$

Based on the profiles of turbulent kinetic energy applied the predictions of pollutants/hazardous gaseous dispersion will also vary. In order to check for horizontal homogeneity a typical case of a flat

terrain which is 5000 m long and 5000 m broad with a boundary layer height of 800 m (z-coordinate) is chosen for investigation [5, 6]. The aerodynamic roughness height is considered to be uniform and set as 0.1 m. The sand grain roughness height corresponding to the aerodynamic roughness height is calculated using the eqn. 21. The sand grain roughness must be set at the wall and has to be accounted for in the standard wall functions used. The pressure-velocity coupling is accomplished using the SIMPLE algorithm and QUICK schemes are used for the discretization of the convective and diffusion terms in the continuity and momentum equations. A grid dependence study is carried out to arrive at the optimal number of elements. A velocity magnitude of 5 m/s at an altitude of 10 m is chosen for the present study. Steady state simulations have been carried out using the standard $k-\varepsilon$ model. The residuals are set as 10^{-06} for the velocity components and the turbulent quantities. The profiles at two different locations (location1: x = 2000 m; y = 2500 m and z = 0 to 800 m: location 2: x = 5000 m; y = 2500 m and z = 0 to 800 m) are retrieved and compared with the inlet profiles. The profiles of the velocity magnitude, turbulent kinetic energy and turbulent dissipation rate are presented in Fig.1. As it can be seen from the profiles of turbulent kinetic energy the values are supposed to remain a constant from the formula $k(z) = \frac{u_*^2}{\sqrt{C_\mu}}$ but there exist a bit of discrepancy as the flow progresses through the

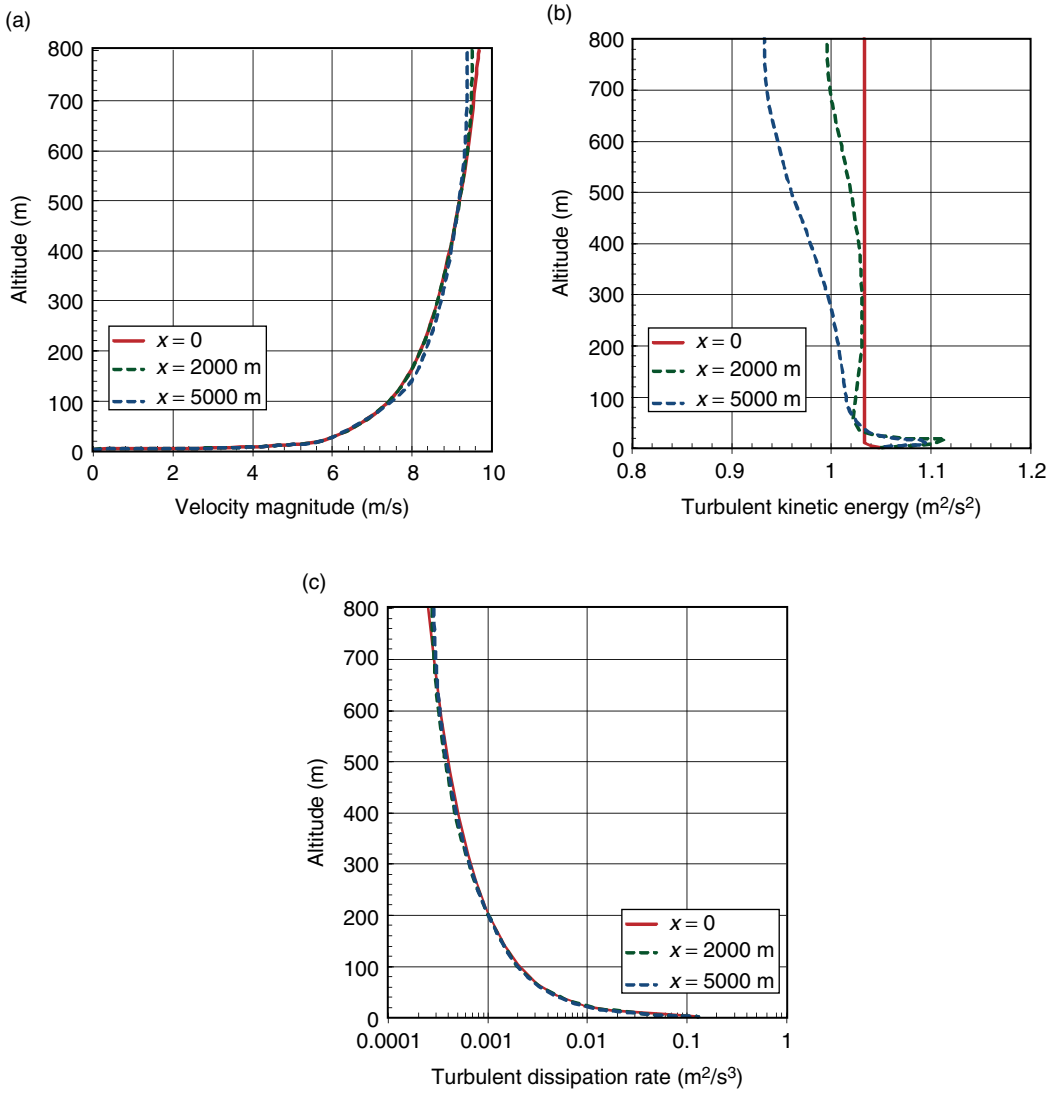

Figure 1. Profiles of the velocity magnitude, turbulent kinetic energy and turbulent dissipation rate.

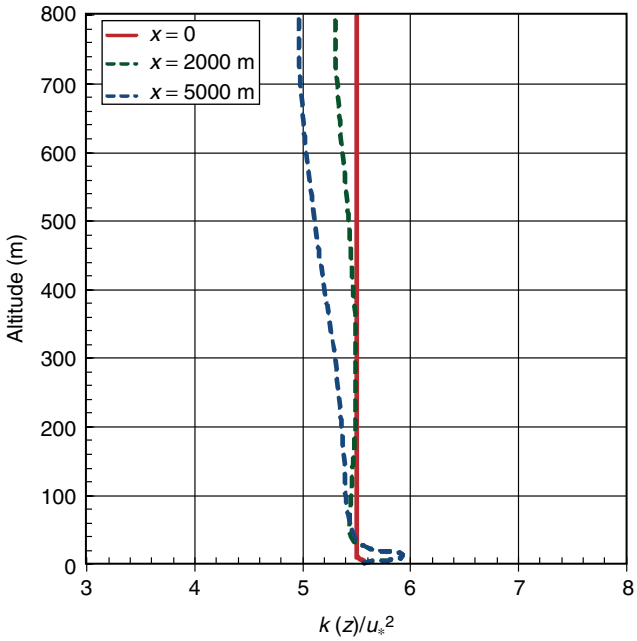

Figure 2. Variation of the parameter $\frac{k(z)}{u_*^2}$ at the inlet and two different locations (x = 2000 m and x = 5000 m).

domain. The sudden jump in the first cell can be attributed to the behavior of the wall function and thereafter it is the heterogeneity of the flow. The turbulent dissipation rate remains almost the same throughout the domain. The value $\frac{k(z)}{u_*^2} \approx 5.5$ and the variation of this parameter is plotted in Fig. 2

It can also be seen from literature that there are studies that assume a different profile for turbulent kinetic energy. In the previous analysis the profile of turbulent kinetic energy was set as a constant whereas in the present analysis the profile of turbulent kinetic energy is given by eqn. (23) which is $k(z) = \frac{u_*^2}{\sqrt{C_\mu}}\left(1 - \frac{z}{\delta}\right)^2$. The domain considered is the same as the one considered in the previous investigation i.e., flat terrain which is 5000 m long and 5000 m broad with a boundary layer height of 800 m (z-coordinate). The profiles at two different locations (location1: x = 2000 m; y = 2500 m and z = 0 to 800 m: location 2: x = 5000 m; y = 2500 m and z = 0 to 800 m) are retrieved and compared with the inlet profiles. The profiles of the velocity magnitude, turbulent kinetic energy and turbulent dissipation rate are presented in Fig. 3.

The profiles of turbulent kinetic energy shows that the value of turbulent kinetic energy is maximum close to the ground and thereafter it decreases and reaches values close to zero at the far outer region. The value $\frac{k(z)}{u_*^2} \approx 5.5$ and the variation of this parameter is plotted in Fig. 4

3.2. Specification of wall shear stress at the ground

Yet another means of specifying the boundary condition would be the imposition of the wall shear stress at the ground. The authors advocate this as the best possible means of ensuring a horizontally homogeneous turbulent boundary layer (HHTBL). The velocity profiles are fully developed throughout the domain and there exist minimal deviation for the imposed profiles on the computation domain. It is clearly evident from the profiles of turbulent dissipation rate that this method is comparatively superior to the ones explained before. Fig. 5 presents the profiles of the velocity magnitude, turbulent kinetic energy and turbulent dissipation rate obtained by specifying the wall shear stress at the ground.

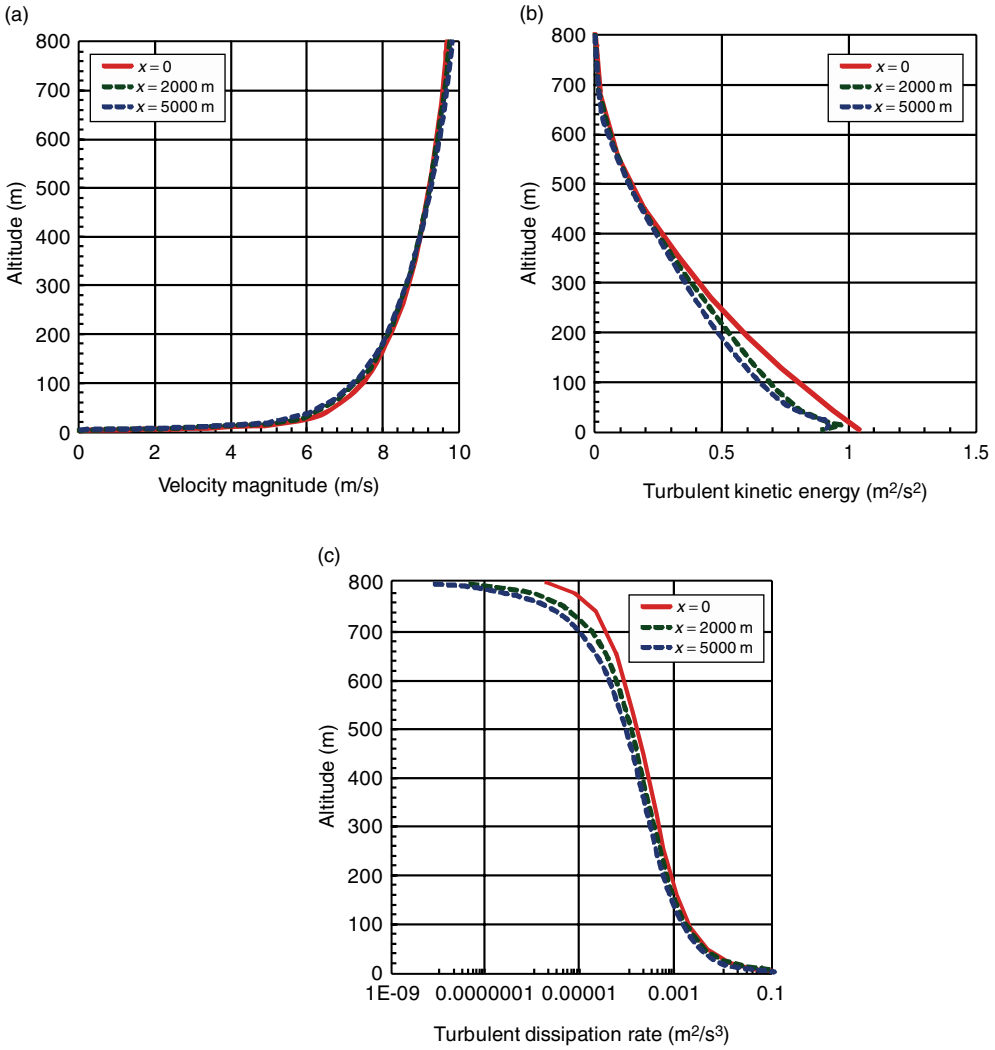

Figure 3. Profiles of velocity magnitude, turbulent kinetic energy and turbulent dissipation rate.

3.3. Reynolds stress model

In the previous studies [5, 6] the Reynolds Stress Model (RSM model) is portrayed as a superior model and is reported to provide results those are far better than those obtained using the two equation models. In the present study, the authors have attempted to probe a bit further into this widely prevalent notion of the superiority of the higher order models over the two equation models for atmospheric flows. There exists a plethora of literature on the various turbulence models and for the sake of brevity the equations related to these models are not presented in the present work. Interested readers are requested to read through the book on turbulence models [10, 11]. In the present investigation the imposed profiles of velocity and turbulent quantities remain the same in both the models (i.e. the $k - \varepsilon$ model and the RSM model). The results obtained using these models are very different and though the RSM solves more number of equations and takes an enormous amount of time for convergence the results are not that promising. The profiles of the velocity magnitude, turbulent kinetic energy and turbulent dissipation rate obtained using the RSM model has been presented in figure 6.

From the cases analyzed so far it is seen that the two equation turbulence model such as the standard $k - \varepsilon$ model itself is good enough for modeling atmospheric boundary layer flows and the specification of the wall shear stress at the ground seem to yield favorable results. The profiles of velocity, turbulent quantities and most importantly temperature are imposed on the computational domain and the horizontal homogeneity in the case of a stably and unstably stratified atmospheric boundary layer flows is verified. The Figs. 7 and 8 present the profiles of velocity magnitude and the turbulent quantities for the stably and unstably stratified BL.

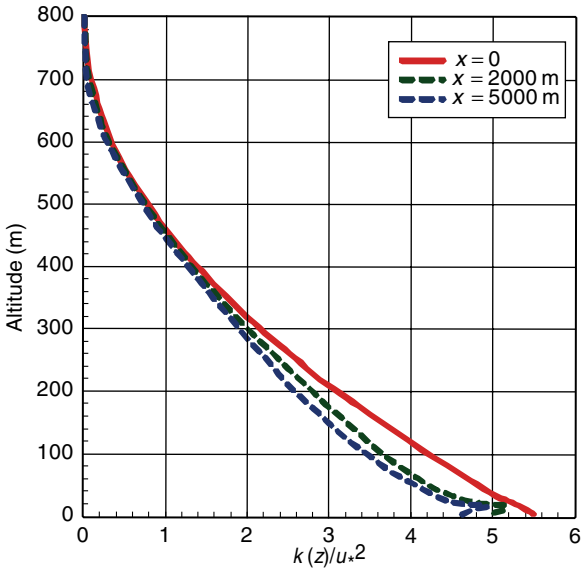

Figure 4. Variation of the parameter $\frac{k(z)}{u_*^2}$ at the inlet and two different locations (x = 2000 m and x = 5000 m).

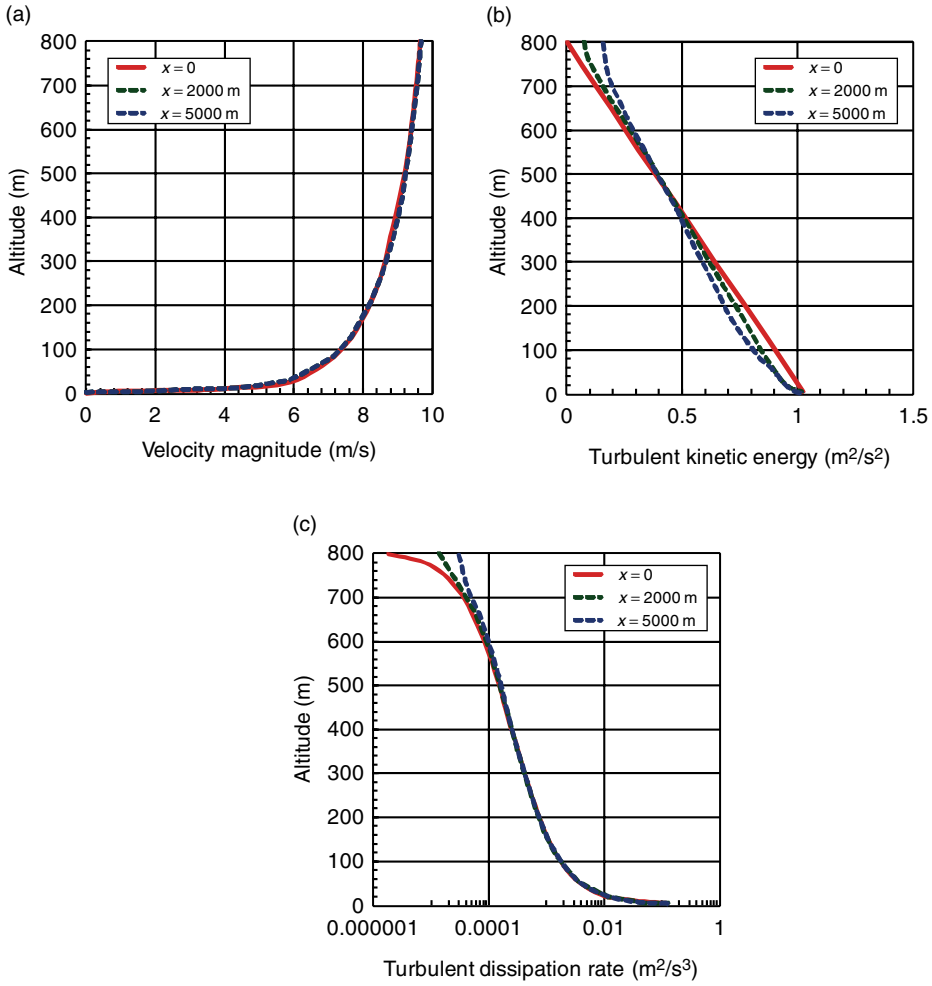

Figure 5. Profiles of velocity magnitude, turbulent kinetic energy and turbulent dissipation rate obtained by the specification of wall shear stress at the ground.

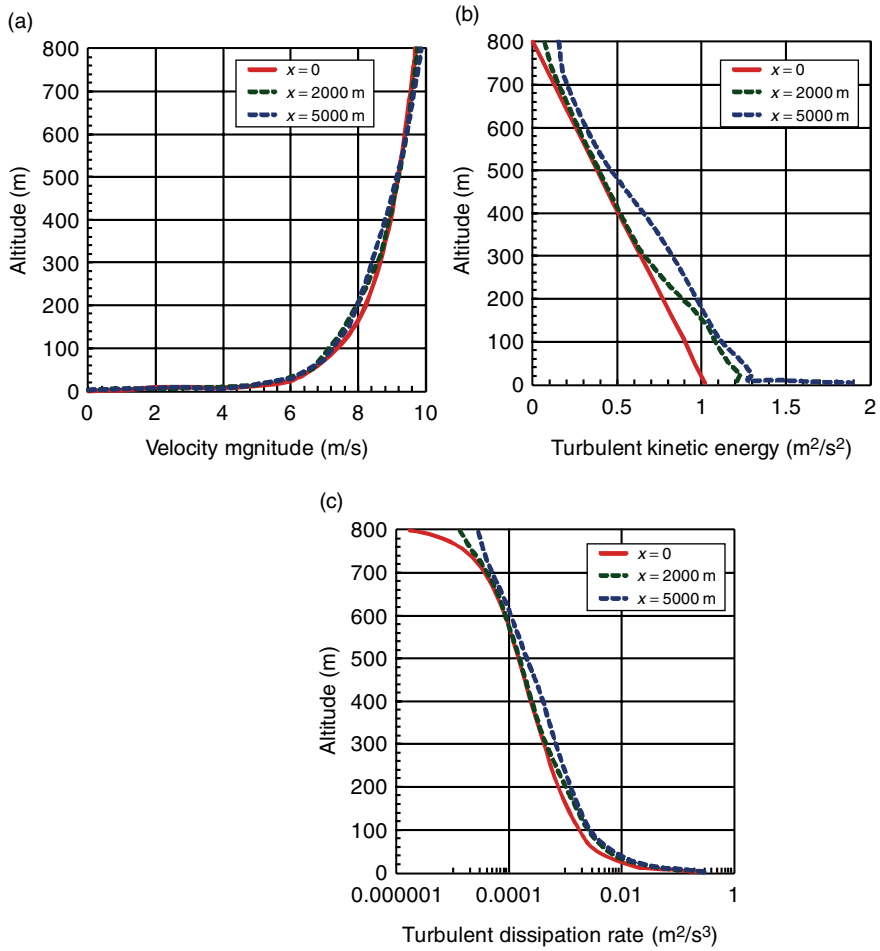

Figure 6. Profiles of velocity magnitude, turbulent kinetic energy and turbulent dissipation rate obtained using the RSM model.

3.4. Prairie grass experiment

The Prairie Grass experiment of 1956 [9] has an undeniable significance in the field of environmental modeling and is quite extensively used in the validation of dispersion models. The Prairie grass experiment was conducted on an experimental site with minimum interference from the surrounding man-made structures. Sulphur-di-oxide was released from a tube which was located at a height of 0.46 m from the ground level and the traces of emitted SO_2 were measured at an arc distance of 50, 100, 200, 400 and 800 meters respectively.

For the present study 4 cases from the Prairie grass experiment have been considered for investigation. Of the 4 cases, two are chosen to represent the neutrally stratified atmospheric condition and the other 2 are truly representative of the stably stratified atmosphere. The Monin Obukhov length given by eqn. (11) is used to differentiate between the neutrally and stably stratified atmospheric conditions. The Monin Obukhov length (L) tends to very high values in neutral stratification and hence is shown as $L \rightarrow \infty$ in the tabular column.

Based on the stability class, the profiles are imposed on the inlet boundary and also inside the whole computational domain serving as a good initial guess for the iteration to progress. One serious limitation of imposing a good guess which is closer to the expected results would be the failure to achieve convergence. In the present study the cases have always converged irrespective of the domain size and number of grid/elements chosen for the analysis. A convergence criterion of 10^{-6} has been set for the continuity, momentum, energy and concentration equations.

The computation domain chosen for the present investigation is 800 m long, 30 m high and 50 m wide. The SO_2 gas is released at a height of 0.46 m from the ground. The ground has a roughness of 0.001 m aerodynamic height. The measurements are available at a height of 1.5 m from the ground. The

Stably Stratified Boundary Layer

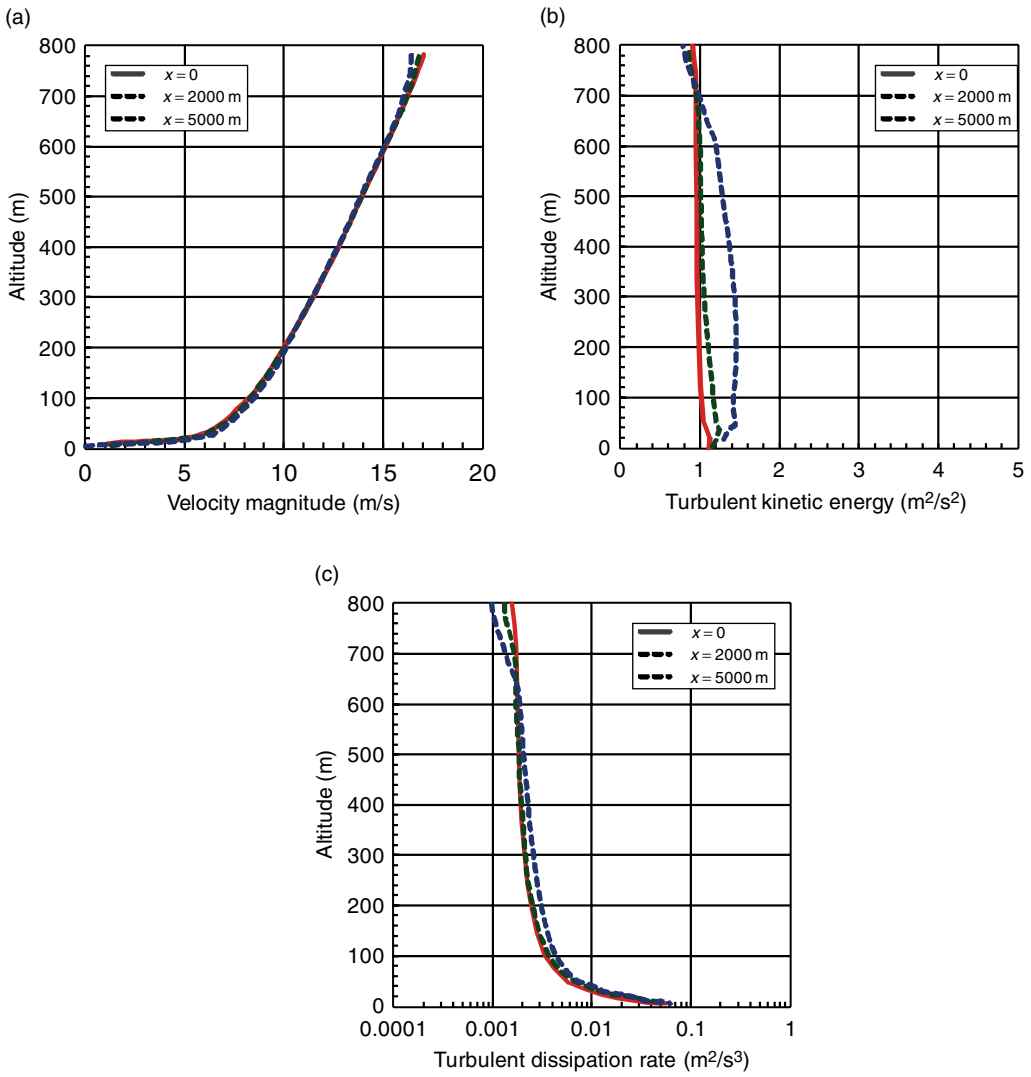

Figure 7. Profiles of velocity magnitude, turbulent kinetic energy and turbulent dissipation rate for a stably stratified BL.

velocity of the released gas and the wind varies considerably from case to case. The wind speed/velocity magnitude is measured at an altitude of 2 m from the ground.

The velocity at the top boundary is specified using eqn. (12). This approach is more suitable for simulating atmospheric flows then specifying a symmetric or a frictionless wall boundary condition at the top. An alternate approach would be to specify the pressure condition at the top. The ground is set as a wall with specified shear stress. This ensures that the HHTBL is achieved and thereby the predictions of concentration profiles are reliable. A grid independence study has been performed using a total cell size of 1.25 million cells and 2.5 million cells respectively. It has been concluded that 1.25 million elements are far more than sufficient for obtaining a reliable or a grid independent solution.

First two cases are categorized as neutrally stratified ones (Monin Obukhov length is quite high) and thereby the profiles for the neutrally stratified atmosphere have been used for the analysis. The measurement for case 1 is available at an angle of 89° from the point of ejection of SO_2 and for case 2 measurements are available at an angle of 57°. Fig. 9 and 10 shows the concentration in mg/m^3 at various locations along the direction of flow. The numerical results for concentration obtained for case 1 and 2 are in good agreement with the experimental data. It is to be noted that for the neutral cases considered for investigation only one set of measurement data is available whereas for cases 3 and 4

Unstably stratified BL

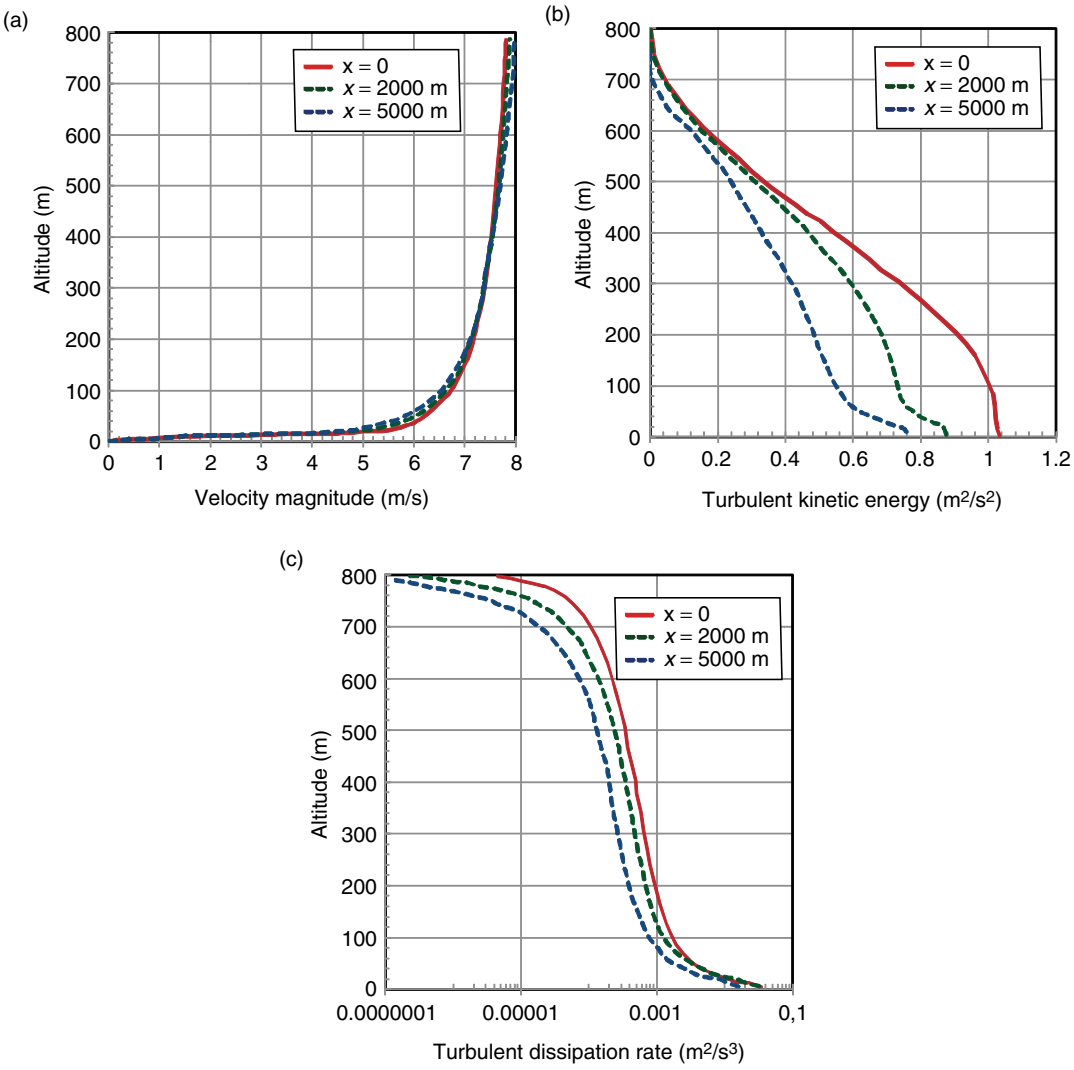

Figure 8. Profiles of velocity magnitude, turbulent kinetic energy and turbulent dissipation rate for an un-stably stratified BL.

Table 2. Prairie grass experimental data for the test cases considered for investigation.

Parameters	Case 1	Case 2	Case 3	Case 4
Release Rate [Kg/s]	0.0565	0.0974	0.0611	0.0405
Release Velocity [m/s]	10.5	18.4	11.1	7.5
Stability Class	Neutral	Neutral	Stable	Stable
Wind Speed at an altitude of 2 m [m/s]	3.3	9.0	1.3	1.9
Ambient temperature [°C]	300.15	304.15	293.15	299.15
Monin Obukhov length [m]	∞	∞	9	9

there are two sets of data points available as measurement were taken on both the directions to the point of SO_2 gas release. There exist a slight discrepancy in the numerical predictions of concentration and the available experimental data for cases 3 and 4. This can be attributed to the anisotropic nature of the ABL flows.

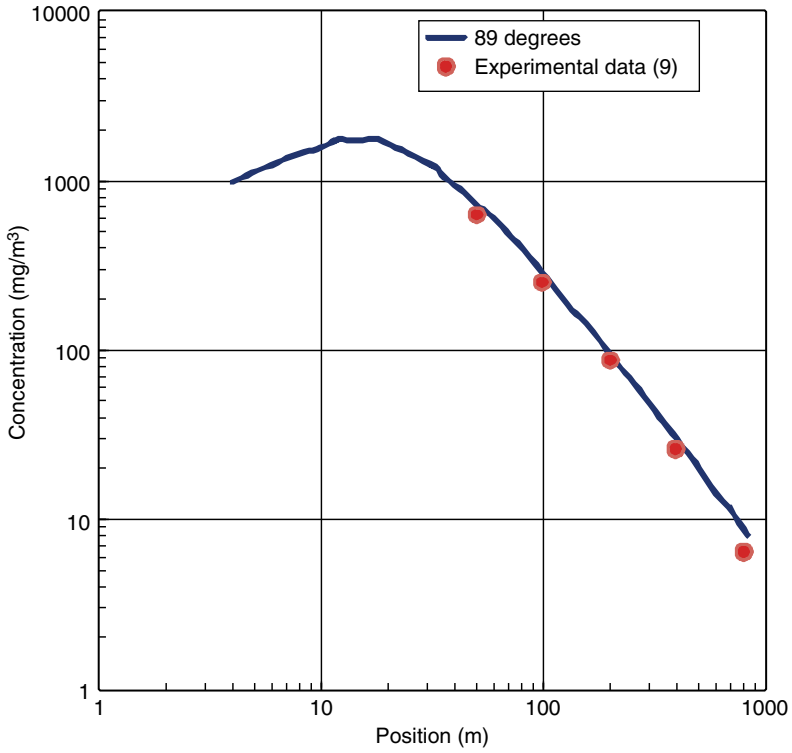

Figure 9. Comparison between the Prairie grass experimental data and the predicted numerical concentrations at various locations for Case 1.

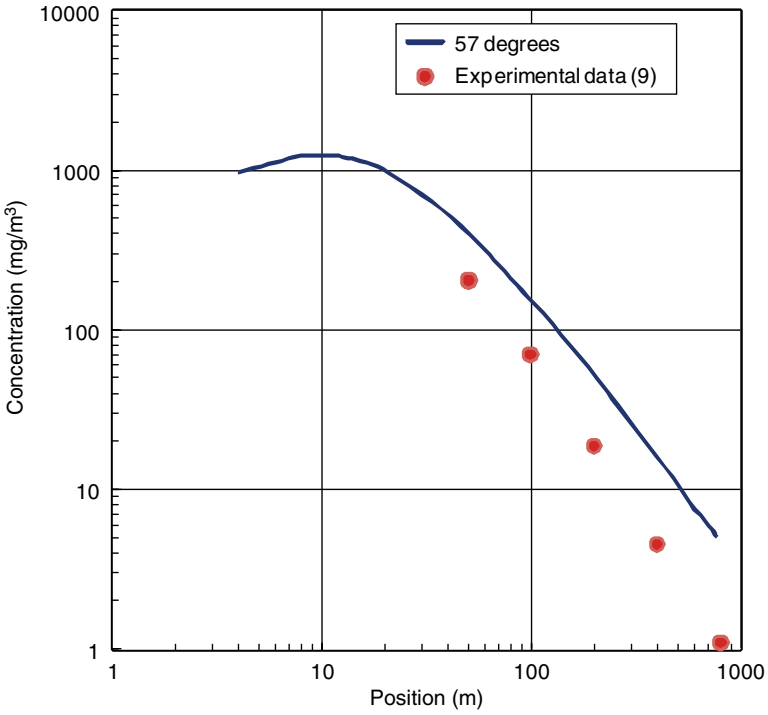

Figure 10. Comparison between the Prairie grass experimental data and the predicted numerical concentrations at various locations for Case 2.

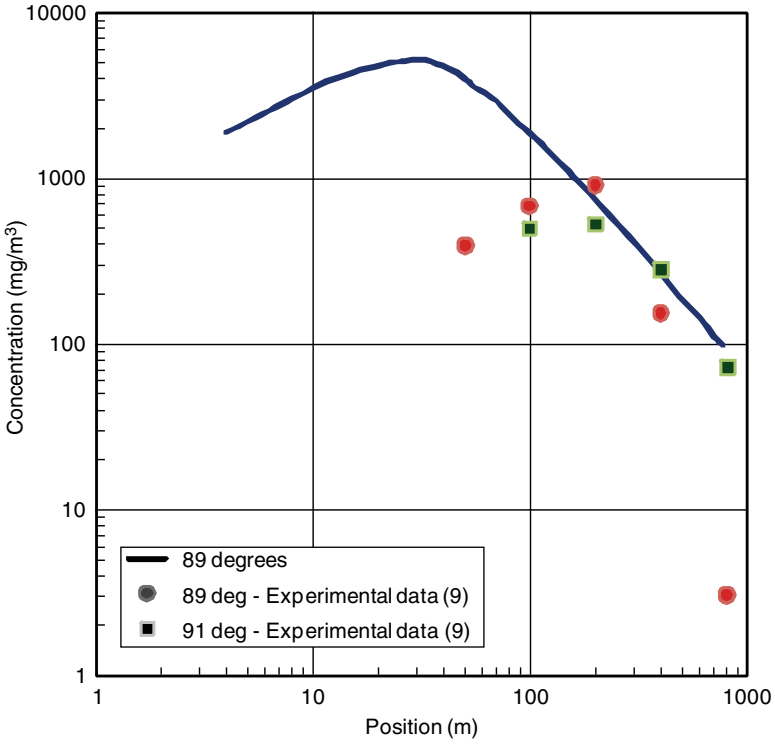

Figure 11. Comparison between the Prairie grass experimental data and the predicted numerical concentrations at various locations for Case 3.

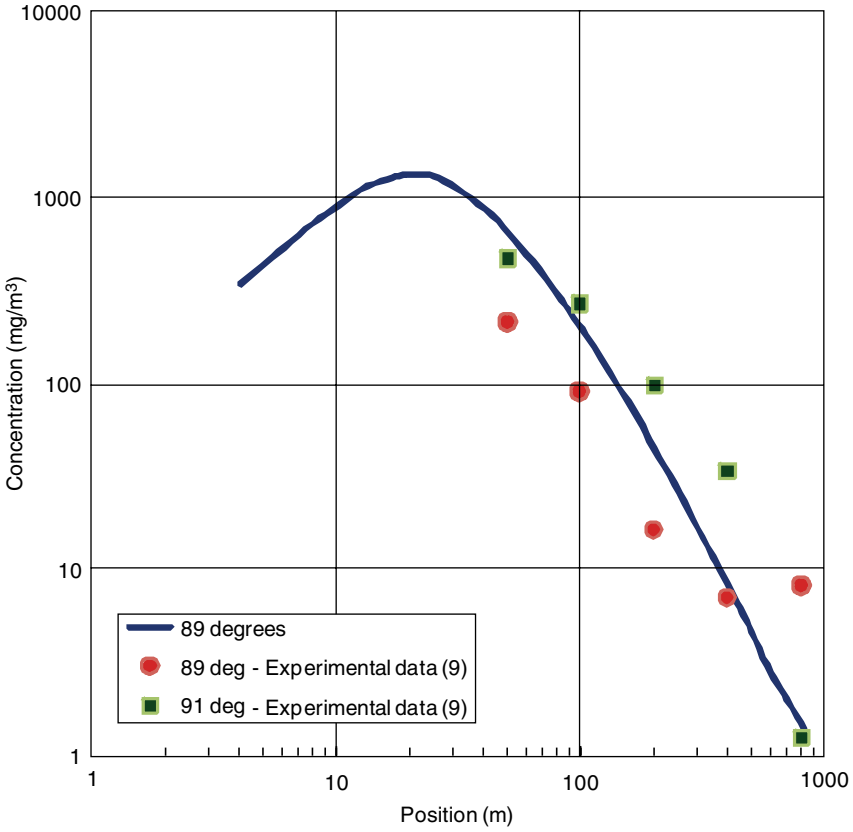

Figure 12. Comparison between the Prairie grass experimental data and the predicted numerical concentrations at various locations for Case 4.

4. CONCLUSIONS

Numerical investigations on hazardous gas dispersion in neutral and stably stratified atmospheric flows have been performed and the results are compared with available experimental data. The profiles of velocity, temperature and turbulence quantities are an absolute necessity in modeling such ABL flows. From the present investigation, it is clearly evident that the specification of the wall shear stress at the ground ensures a horizontally homogeneous turbulent boundary layer (HHTBL). It is also seen that the two equation turbulence model along with the convection diffusion equation to model concentration distribution, itself is sufficiently good enough for predicting the concentration of dispersed gases in a large computational domain. Future studies will be focused on the application of the implemented model for predicting pollutant cum hazardous gas dispersion in urban environment.

REFERENCES

[1] Hargreaves. D. M, Wright. N.G. On the use of the k-ε model in commercial CFD software to model the neutral atmospheric boundary layer. Journal of Wind Engineering and Industrial Aerodynamics. 2007; 95: 355–369.

[2] Hargreaves. D. M, Wright. N.G. The use of commercial CFD software to model the atmospheric boundary layer. The Fourth International Symposium on Computational Wind Engineering CWE 2006. Yokohama.

[3] Palma. J.M.L.M, Crasto. F.A, Ribeiro. L.F, Rodrigues. A.H, Pinto. A.P. Linear and nonlinear models in wind resource assessment and wind turbine micro-siting in complex terrain. Journal of Wind Engineering and Industrial Aerodynamics. 2008; 96: 2308–2326.

[4] Ramechecandane. S, Arne R Gravdahl. Numerical investigations on wind flow over complex terrain. Wind Engineering. 2012; 3: 273–296.

[5] Riddle. A, Carruthers. D, Sharpe. A, McHugh. C, Stocker. J. Comparisons between FLUENT and ADMS for atmospheric dispersion modeling. Atmospheric Environment. 2004; 38: 1029–1038.

[6] Di Sabatino. S, Buccolieri. R, Pulvirenti. B, Britter. R.E. Flow and pollutant dispersion in street canyons using FLUENT and ADMS-Urban. Environmental Modelling and Assessment. 2008; 13: 369–381.

[7] Vendel. F, Lamaison. G, Soulhac. L, Volta. P, Donnat. L, Duclaux. O, Puel. C. Modelling diabatic atmospheric boundary layer using a RANS CFD code with a k-epsilon turbulence closure. 13th Conference on Harmonisation within Atmospheric Dispersion Modelling for Regulatory Purposes. HARMO–13, 1–4 June 2010, Paris, France.

[8] Duynkerke. P.G. Application of the E-ε turbulence closure model to the neutral and stable atmospheric boundary layer. Journal of the atmospheric sciences. 1988; 45(5): 865–880.

[9] Barad, M.L. Project Prairie Grass, a field program in diffusion. Geophys. Res. Pap. 59. Vol 1, Report AFCRC-TR-58-235, Air Force Cambridge Centre. 1958

[10] Tennekes. H, Lumley, J.L. A First Course in Turbulence. MIT press, 1972.

[11] Tuncer Cebecci. Turbulence Models and Their Application: Efficient Numerical Methods with Computer Programs. Springer, 2004.